JCI The Journal of Clinical Investigation

Functional selectin ligands mediating human CD34$^+$ cell interactions with bone marrow endothelium are enhanced postnatally

Andrés Hidalgo, … , Linnea A. Weiss, Paul S. Frenette

J Clin Invest. 2002;110(4):559-569. https://doi.org/10.1172/JCI14047.

Article

Hematopoietic progenitor cells (HPCs) can home to the bone marrow (BM) after a simple intravenous injection, but the adhesive mechanisms mediating the initial interactions of human HPCs with the BM endothelium have not been evaluated in vivo. Using fluorescence intravital microscopy and homing assays in NOD/SCID mice, we show that endothelial selectins are necessary for human adult CD34$^+$ cell homing, since rolling on BM endothelium and retention in the BM compartment are drastically reduced (>90%) in endothelial selectin–deficient NOD/SCID mice. Comparative analyses of CD34$^+$ cells collected from adults and from cord blood (CB) reveal that neonatal cells display reduced rolling fractions compared with adult CD34$^+$ cells obtained from peripheral blood or BM, suggesting abnormal selectin ligand function on neonatal progenitors. Flow cytometric and intravital microscopy studies suggest that this defect results from nonfunctional P-selectin ligand on a subset (~30%) of neonatal CD34$^+$ cells. Further analyses indicate that P-selectin glycoprotein ligand-1 (PSGL-1) is expressed in a nonfunctional form among neonatal CD34$^+$ cells that do not bind P-selectin and that this subset is enriched in primitive CD34$^+$CD38$^{lo/-}$ progenitors. These results underscore the potential to improve homing of CB CD34$^+$ cells to the BM by manipulation of selectins and their ligands.

Functional selectin ligands mediating human CD34$^+$ cell interactions with bone marrow endothelium are enhanced postnatally

Andrés Hidalgo, Linnea A. Weiss, and Paul S. Frenette

Department of Medicine, Mount Sinai School of Medicine, New York, New York, USA

Hematopoietic progenitor cells (HPCs) can home to the bone marrow (BM) after a simple intravenous injection, but the adhesive mechanisms mediating the initial interactions of human HPCs with the BM endothelium have not been evaluated in vivo. Using fluorescence intravital microscopy and homing assays in NOD/SCID mice, we show that endothelial selectins are necessary for human adult CD34$^+$ cell homing, since rolling on BM endothelium and retention in the BM compartment are drastically reduced (>90%) in endothelial selectin–deficient NOD/SCID mice. Comparative analyses of CD34$^+$ cells collected from adults and from cord blood (CB) reveal that neonatal cells display reduced rolling fractions compared with adult CD34$^+$ cells obtained from peripheral blood or BM, suggesting abnormal selectin ligand function on neonatal progenitors. Flow cytometric and intravital microscopy studies suggest that this defect results from nonfunctional P-selectin ligand on a subset (~30%) of neonatal CD34$^+$ cells. Further analyses indicate that P-selectin glycoprotein ligand-1 (PSGL-1) is expressed in a nonfunctional form among neonatal CD34$^+$ cells that do not bind P-selectin and that this subset is enriched in primitive CD34$^+$CD38$^{lo/-}$ progenitors. These results underscore the potential to improve homing of CB CD34$^+$ cells to the BM by manipulation of selectins and their ligands.

J. Clin. Invest. **110**:559–569 (2002). doi:10.1172/JCI200214047.

Introduction

Hematopoietic progenitor cells (HPCs) can be transplanted to the bone marrow (BM) of another individual following a simple intravenous infusion. The ability of HPCs to home to the BM was first demonstrated a few decades ago when Jacobson and colleagues showed that shielding of the spleen allowed mice to recover from a lethal dose of radiation (1). This study, along with others (2, 3), established that pluripotent stem cells present in the spleen or infused exogenously could repopulate distant hematopoietic organs. This feature is the basis for the clinical use of BM transplantation in treatment of hematologic malignancies (4). However, despite an advanced knowledge of the mechanisms that allow the migration of mature leukocytes into inflamed tissues, the mechanisms of human HPC homing to the BM are still poorly understood.

Received for publication August 23, 2001, and accepted in revised form June 24, 2002.

Address correspondence to: Paul S. Frenette, Mount Sinai School of Medicine, One Gustave L. Levy Place, Box 1079, New York, New York 10029, USA. Phone: (212) 659-9693; Fax: (212) 849-2574. E-mail: paul.frenette@mssm.edu.

Conflict of interest: No conflict of interest has been declared.

Nonstandard abbreviations used: hematopoietic progenitor cell (HPC); bone marrow (BM); P-selectin glycoprotein ligand-1 (PSGL-1); mobilized peripheral blood (mPB); cord blood (CB); phycoerythrin (PE); low-density mononuclear cell (MNC); red blood cell (RBC); carboxyfluorescein succinimidyl ester (CFSE); P- and E-selectin null (P/E$^{-/-}$); enhanced green fluorescent protein (EGFP); transgenic (Tg); intravital microscopy (IVM).

The migration of leukocytes to sites of inflammation is initiated by labile but critical adhesive interactions (attachment and rolling) that are largely mediated by the selectin family and its glycoconjugated ligands. Two members of the selectin family, P- and E-selectins, are expressed on endothelial cells (5, 6). P-selectin is stored in granules of endothelial cells and platelets and is rapidly translocated to the cell surface after stimulation with various secretagogues. E-selectin expression is induced by endotoxin or inflammatory cytokines. Although the E-selectin gene is silent in cultured endothelial cells, low levels of E-selectin are expressed in most tissues in vivo and regulate leukocyte homeostasis together with endothelial P-selectin (7). Mice lacking both P- and E-selectins display severe leukocytosis and can develop spontaneous skin infections (7, 8). The main ligand for P-selectin, P-selectin glycoprotein ligand-1 (PSGL-1), is a disulfide-bonded homodimeric mucin-like glycoprotein expressed on leukocytes (9), platelets (10), and CD34$^+$ cells (11, 12). PSGL-1 requires specific posttranslational modifications in order to be functional. These include sialylation and fucosylation of O-linked sugars, as well as sulfation of tyrosine residues present in the N-terminus of the protein (13). While P- and E-selectin are critical for myeloid cell rolling in venules of the systemic circulation, the leukocyte selectin (L-selectin) mediates lymphocyte rolling in specialized venules of secondary lymphoid organs. The close interaction between leukocytes and endothelial cells during the rolling step allows the activation of leukocyte integrins triggered

by chemokines present on the surface of the endothelium. This leads to the firm adhesion and migration of leukocytes through the vessel wall into the extravascular space (14). Whether a similar paradigm is applicable for immature hematopoietic precursors is still unclear. However, studies in mice suggest that the recruitment of HPCs into the BM requires multiple adhesion pathways, including endothelial selectins and VCAM-1 (15–18).

The study of primitive human hematopoiesis in vivo has been facilitated by the generation of NOD/LtSz-scid/scid mice (hereafter referred to as NOD/SCID mice) that have multiple defects in innate and adaptive immunologic functions (19). The BM of NOD/SCID mice can be repopulated by human HPCs ($CD34^+$ cells) after sublethal doses of radiation (20). Clinically, human HPCs are obtained from three different sources: BM, mobilized peripheral blood (mPB), and cord blood (CB). CB-derived progenitors represent an especially promising source of human hematopoietic stem cells because they are widely available and their use is associated with reduced graft-versus-host disease (21). However, transplantation using CB cells has been restricted mostly to children due to the limited number of cells available in the placenta (22).

Here, we describe the molecular mechanisms mediating the initial adhesive interactions of human HPCs in the BM microcirculation of NOD/SCID mice using fluorescence intravital microscopy. We show that human $CD34^+$ cell rolling on BM endothelium and extravasation into the BM compartment are completely dependent upon endothelial selectins. In addition, we demonstrate that the initial interactions of CB $CD34^+$ cells are reduced compared with those derived from adult sources. We show that a large subset (~30%) of neonatal $CD34^+$ cells, enriched in primitive $CD34^+CD38^{lo/-}$ cells, does not bind P-selectin, and that this inability to bind P-selectin originates from incomplete posttranslational modifications of PSGL-1. These results may have implications for therapies using CB progenitor/stem cells.

Methods

Ab's and selectin chimeras. For in vivo studies, rat mAb's against mouse VCAM-1 (MK 2.7) and P-selectin (clone RB40.34) were purified from hybridoma supernatants (American Type Culture Collection, Rockville, Maryland, USA), and control rat IgG was obtained from Sigma-Aldrich (St. Louis, Missouri, USA). Potential endotoxin contamination was removed using a polymyxin B column (Detoxi-Gel; Pierce Biotechnology Inc., Rockford, Illinois, USA). The rat anti–mouse E-selectin Ab (clone 9A9) was a generous gift of B. Wolitzky (MitoKor, San Diego, California, USA). Anti–human PSGL-1 (KPL1) and FITC-conjugated anti–human CD38 were purchased from Pharmingen (San Diego, California, USA), and phycoerythrin-conjugated (PE-conjugated) anti–human CD34 (clone AC136) was from Miltenyi Biotec (Bergisch Gladbach, Germany). The mouse anti–human PSGL-1 Ab (PSL-275) and human P-selectin–IgG chimera were generously provided by R. Schaub (Genetics Institute, Cambridge, Massachusetts, USA). Murine E- and P-selectin–IgM chimeras were produced by transfection of COS-7 cells with selectin-IgM DNA vector (a kind gift of John Lowe, University of Michigan, Ann Arbor, Michigan, USA) using the DEAE-dextran method (23).

Human samples and $CD34^+$ cell isolation. Fresh human hematopoietic cell samples were obtained from unused portions of three different clinical sources: steady-state BM, mPB, and CB. BM samples were collected from normal donors at the time of harvest for allogeneic transplantation. mPB cells were collected by leukapheresis from either healthy donors (n = 19) or patients with hematopoietic malignancies in remission (n = 15). Both BM and mPB samples were obtained from the Mount Sinai Bone Marrow Transplantation Program. Umbilical CB samples were obtained from normal full-term deliveries (≥38 weeks). All human samples were obtained in accordance with protocols approved by the Internal Review Board of Mount Sinai.

For the enrichment of $CD34^+$ cells, low-density mononuclear cells (MNCs) were collected after centrifugation at 250 g over Ficoll-Hypaque (d = 1.077 g/ml). After two washes in PBS containing 2 mM EDTA and 0.5% BSA, contaminating red blood cells (RBCs) were lysed in a 0.8% NH_4Cl solution. $CD34^+$ cells were purified from the MNC fraction using the CD34-isolation mini-MACS kit (Miltenyi Biotec) following the manufacturer's instructions. The purity of the isolated $CD34^+$ cells ranged from 70% to 99% (average ~89% for CB and ~95% for mPB). For intravital microscopy experiments, purified human $CD34^+$ cells were fluorescently labeled by incubation with 33 μM carboxyfluorescein succinimidyl ester (CFSE; Molecular Probes Inc., Eugene, Oregon, USA) for 30 minutes at room temperature and washed three times in RPMI before injection into mice via the carotid artery catheter.

Mice. A NOD/SCID mouse colony was established from breeding pairs obtained from The Jackson Laboratory (Bar Harbor, Maine, USA). Mice with P- and E-selectin double null mutations ($P/E^{-/-}$) or a single E-selectin null mutation ($E^{-/-}$) (7) were backcrossed into the NOD/SCID background. After each generation, blood counts were monitored to select for the SCID mutation. Third generation littermates, which display a lymphopenia similar to that in pure NOD/SCID animals, were used to set up colonies of selectin knockouts and control wild-type NOD/SCID mice. Wild-type and selectin-deficient NOD/SCID mice had numbers of T ($CD3^+$) cells, B ($B220^+$) cells, and NK ($NK1.1^+$) cells similar to the parental NOD/SCID pure strain as assessed by FACS analysis of the peripheral blood and BM. Transgenic mice expressing the enhanced green fluorescent protein under the control of the β-actin promoter (EGFP-Tg mice; a kind gift from M. Okabe, Osaka University, Japan) were bred

in the barrier facility at Mount Sinai School of Medicine. Mice were fed with sterilely irradiated chow and autoclaved water. Experimental procedures on animals were approved by the Animal Care and Use Committee at the Mount Sinai School of Medicine.

Intravital microscopy of the BM. Mice 6–9 weeks old were used for BM intravital microscopy (BM-IVM). To avoid the retention of injected human cells in the spleen, mice were splenectomized upon weaning as described (16) and allowed to recover for at least 2 weeks before BM-IVM experiments. Mice were anesthetized by intraperitoneal injection (6 ml/kg) of 100 mg/ml urethane and 20 mg/ml chloralose (both from Sigma-Aldrich) in PBS. This anesthetic combination was chosen because it does not significantly alter blood flow in the BM microcirculation. The hair in the submandibular area of the neck and on the skullcap was removed using a hair removal lotion (Nair; Carter Products, New York, New York, USA). The trachea was cannulated with PE-160 polyethylene tubing to facilitate spontaneous respiration, and a PE-10 catheter (Becton, Dickinson and Co., Franklin Lakes, New Jersey, USA) was inserted into the left common carotid artery for injection of fluorescent cells and Ab's. The scalp was incised in the midline to expose the frontoparietal skull, and the conjunctive tissue covering the skull was carefully removed. A plastic ring was inserted in the incision area to allow application of endotoxin-free PBS. The mouse's cranium was kept in place using a stereotactic holder (David Kopf Instruments, Tujunga, California, USA). A mouse thus prepared was positioned under a fixed-stage, custom-designed intravital microscope (MM-40) equipped with a mercury fluorescent lamp and water immersion objectives (Nikon Corp., Tokyo, Japan). To block potential sites of retention of human cells, 10^7 unlabeled human MNCs from each sample were injected immediately before the injection of labeled $CD34^+$ cells. Human $CD34^+$ cells are rapidly cleared (within minutes) from the circulation of NOD/SCID mice after injection. Approximately 1×10^6 to 2×10^6 $CD34^+$ cells were injected per experiment to visualize 50–500 cells in the left parietal BM using a 10× water-immersion objective (0.3 NA; Nikon Corp.). For determination of the hemodynamic parameters, 10^7 CFSE-labeled human MNCs or RBCs were injected into the carotid artery at the end of each experiment. In the experiments designed to determine the role of VCAM-1 or P-selectin, mice were preinjected with control rat IgG (or no IgG in two experiments), followed by labeled human $CD34^+$ cells. When cells from the first injection were no longer detected in the circulation (10–15 minutes), the same mouse was injected with anti–VCAM-1 (80 μg) or anti–P-selectin (60 μg) at least 15 minutes before a second injection of labeled human $CD34^+$ cells. In the experiments aimed at evaluating the role of PSGL-1, fluorescently labeled $CD34^+$ cells were incubated with 2 μg KPL1 or control IgG per 10^6 cells prior to intracarotid injection. The images were captured using an SIT camera with a C2400 camera controller (Hamamatsu, Hamamatsu City, Japan) and were recorded using a VHS video recorder (SV0-9500MD; Sony Corp., Tokyo, Japan).

Image analysis. Vessel diameter and cell velocities were measured using a video caliper and sequential single-frame analysis. The maximal velocity (V_{max}), which represents the average velocity of free-flowing CFSE-labeled $CD34^-$ cells or RBCs, was determined for each BM vessel. The mean blood flow velocity (V_{mean}) was thus calculated as $V_{mean} = V_{max}/(2 - \varepsilon^2)$, where ε is the ratio of the $CD34^+$ cell diameter (~7 μm) to the vessel diameter (D_v). The wall shear rate and critical velocity (V_{crit}) were obtained from the following formulas: wall shear rate = $8(V_{mean}/D_v)$, and $V_{crit} = V_{mean} \times \varepsilon(2 - \varepsilon)$. Any cell traveling below V_{crit} was considered to be rolling on the vessel wall. Cells that remained stationary for 5 seconds or more were considered arrested.

Flow cytometry and selectin chimera binding assay. For double staining of CD34 and P-selectin ligands, 10^6 total CB or mPB MNCs depleted of RBCs were washed and resuspended in staining buffer (RPMI, 5% FCS, and 0.02% NaN_3). Fc receptors were blocked with 1 μg human IgG (Sigma-Aldrich), and cells were incubated with PE-conjugated anti–human CD34. After one wash, cells were incubated with 4 μg of the HUMAN P-selectin–IgG chimera that had been preconjugated with 0.3 μg biotinylated protein A. Preliminary experiments showed that this concentration saturates P-selectin ligands on $CD34^+$ cells. Cells were subsequently incubated with an excess of streptavidin-FITC (1.5 μg; Jackson ImmunoResearch Laboratories Inc., West Grove, Pennsylvania, USA) and washed once before analysis using a FACSCalibur flow cytometer (Becton, Dickinson and Co.). All incubations were performed for 20 minutes at 6°C. For triple-color labeling with anti-CD34–PE, P-selectin–IgG–Cy5, and anti-CD38–FITC, the procedure was the same except that an anti-CD38–FITC Ab (Pharmingen) was coincubated with an excess of streptavidin-Cy5 (Jackson ImmunoResearch Laboratories Inc.) before the final wash. In control samples, staining was carried out in the presence of 5 mM EDTA. For double staining of CD34 and PSGL-1, CB or mPB MNCs prepared as described above were incubated with an anti–PSGL-1 Ab (PSL-275 or KPL1), washed once, and incubated with an FITC-conjugated anti-mouse Ab (Pharmingen). After washing, cells were incubated with 1 μg mouse IgG (Sigma-Aldrich) and anti-CD34–PE Ab, washed, and analyzed by flow cytometry. To evaluate E-selectin ligand expression, 10^5 CB- or mPB-derived $CD34^+$ cells were incubated with supernatants from COS-7 cells transfected with the murine E-selectin–IgM construct, followed by PE-labeled anti-human IgM goat Ab (Sigma-Aldrich). A similar procedure was followed for the detection of P-selectin ligands using the murine P-selectin–IgM chimera, using supernatants from COS-7 cells transfected with the murine P-selectin–IgM construct.

Engraftment of EGFP progenitors in the cranial BM and homing of human cells into NOD/SCID femoral BM. To map the areas of hematopoiesis in the calvaria, BM nucleated

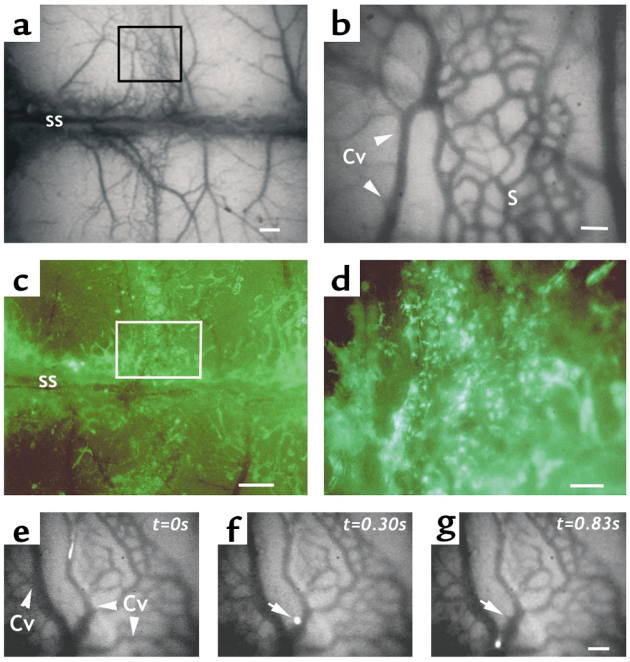

Figure 1
Intravital microscopy of the parietal BM in NOD/SCID mice. (**a**) Low-power view (2× objective) of the murine parietal bone. The sagittal suture (SS), which joins both parietal bones, appears dark due to the blood circulating in the underlying sagittal sinus. The midparietal area (box) viewed at higher magnification (10× objective) in (**b**) represents the area of the parietal bone typically used for the IVM recordings. This area comprises several collecting venules (Cv) and sinusoids (S). (**c** and **d**) Engraftment of the NOD/SCID skull microvasculature with BM nucleated cells from EGFP-Tg mice. Sublethally irradiated NOD/SCID mice were transplanted with BM nucleated cells from EGFP-Tg mice. (**c**) Two weeks after injection, donor cells have engrafted the parasagittal regions and also the midparietal area (box) shown at higher magnification in (**d**). Note that the microvessels are masked by green fluorescent hematopoietic cells. (**e**–**g**) Human $CD34^+$ cell rolling in a NOD/SCID collecting venule. CFSE-labeled $CD34^+$ cells purified from mPB samples were injected via the carotid artery and visualized (10× objective) in the midparietal area of a NOD/SCID mouse. (**e**) A free-flowing $CD34^+$ cell (t = 0 s) in the central Cv (**f**) tethers to the vessel wall (0.30 s), and (**g**) rolls during the following 0.53 seconds. The white arrow marks the initial site of interaction. Supplemental data of a video depicting the BM intravital microscopy model can be downloaded at http://www.jci.org/cgi/content/full/110/4/559/DC1. Bars in **a** and **c**, 500 μm; bars in **b**, **d**, and **g**, 100 μm.

cells (10^6 cells) from F1 generation EGFP-Tg NOD/SCID mice were injected into sublethally irradiated (300 cGy) NOD/SCID recipients. Fourteen days after transplantation, recipient mice were prepared for fluorescence BM-IVM of the parietal bone as described above.

For homing assays, MNCs were isolated from mPB samples as indicated above and resuspended in RPMI. Irradiated (375 cGy) wild-type and $P/E^{-/-}$ NOD/SCID mice were injected intravenously with 2×10^7 MNCs immediately after irradiation. Two hours after injection, mice were sacrificed and femoral BM cells were harvested. After lysis of RBCs and blocking of Fc receptors with mouse and human IgG, 10^6 total BM nucleated cells were stained with both PE-conjugated anti-CD34 and FITC-conjugated anti-CD45 Ab's (Immunotech, Marseilles, France). Flow cytometry was gated on the lymphocyte population since more than 90% of $CD34^+$ cells fall in this region. Analyses were performed on 5×10^5 events per transplanted animal.

Engraftment of human $CD34^+$ cells into NOD/SCID mice. $CD34^+$ cells (10^5) purified from CB or G-CSF mPB were injected intravenously into sublethally irradiated (350–375 cGy) NOD/SCID or β2 microglobulin–deficient NOD/SCID mice (The Jackson Laboratory). Mice were sacrificed 4 weeks after injection. After lysis of RBCs and blocking of Fc receptors with mouse and human IgG, 10^6 BM nucleated cells were stained with an FITC-conjugated anti–human CD45 Ab (Immunotech). Depending on the level of engraftment found by FACS analysis, 0.25×10^5 to 2.5×10^5 BM nucleated cells were plated into methylcellulose media (MethoCult H4433; Stem Cell Technologies, Vancouver, Canada) and incubated at 37°C in a humidified atmosphere containing 5% CO_2. Human myeloid colonies, erythroid colonies, and colonies containing both myeloid and erythroid cells were counted on day 14.

Statistical analysis. All values are reported as mean ± SEM. Statistical significance for two paired or unpaired groups was assessed by the Student t test. The Mann-Whitney test was used to determine statistical significance in engraftment studies.

Results

Human $CD34^+$ cells roll and arrest in NOD/SCID BM microvessels. The thin cortex of murine cranial bones allows one to observe the behavior of fluorescently labeled cells in the BM of living animals using epifluorescence intravital microscopy (17). Because of the protection afforded by the surrounding bone, the BM microvasculature can be observed without direct injury from the surgical preparation. The bulk of cranial BM is concentrated around the bone sutures of the calvaria. However, individual BM microvessels are not clearly visible in most areas by fluorescence intravital microscopy except for a section in the middle of the parietal bone (Figure 1a, box), which displays a well-defined vascular network composed of sinusoids (Figure 1b, "S", honeycomb appearance) draining into at least two collecting venules that run perpendicular or parallel to the sagittal sinus (Figure 1b, Cv, and Figure 1, e–g). The blood flow in the midparietal area of the NOD/SCID BM is centripetal, draining into the sagittal sinus. To evaluate the distribution of active hematopoiesis in the calvaria, BM nucleated cells from EGFP-Tg mice were transplanted into sublethally irradiated (300 cGy) NOD/SCID recipient mice. Fourteen days after transplantation, EGFP-expressing hematopoietic cells had heavily repopulated the parasagittal areas of the parietal bone (including the aforementioned midparietal section; Figure 1, c and d), but also areas in the frontal and occipital bones near

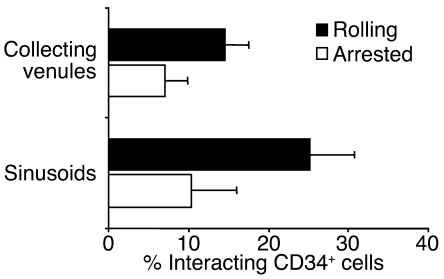

Figure 2
Human CD34⁺ cell rolling and arrest in collecting venules and sinusoids of the BM in NOD/SCID mice. CFSE-labeled human CD34⁺ cells purified from mPB were injected into NOD/SCID mice, and the fractions of cells rolling or arrested in collecting venules or sinusoids were determined by IVM analysis of videotapes. Bars represent mean ± SEM. The differences between Cv and sinusoids for the number of rolling and arrested cells are not significant (P = 0.14 and 0.6, respectively). n = 7 different human donors and the same number of mice.

the coronal and lambdoidal sutures, respectively (not shown). These results indicate that the midparietal area carries active hematopoiesis and that the distribution of hematopoietic sites in the cranium of NOD/SCID animals is similar to that described in C57BL/6 animal studies using rhodamine 6G uptake (17).

Having established that the midparietal vascular network in NOD/SCID mice encompasses BM tissue, we next set out to evaluate the behavior of human HPCs in the BM microcirculation. CD34⁺ cells from G-CSF–mobilized healthy donors or from patients with hematologic malignancies in remission were isolated. Purified CD34⁺ cells were fluorescently labeled and injected via the carotid artery of NOD/SCID mice prepared for intravital microscopy. Labeled cells can be individually tracked in BM microvessels (Figure 1, e–g) and the percentages of rolling and arrested cells determined by careful analysis of video recordings. To comparatively evaluate CD34⁺ cell interactions in sinusoids and collecting venules, we initially studied the numbers of rolling and arrested HPCs in each vessel type separately. Although there was a trend toward a larger CD34⁺ cell rolling fraction in sinusoids compared with collecting venules, the difference was not significant (Figure 2; P = 0.14). Therefore, the numbers of rolling and arrested cells in both types of microvessels were pooled in subsequent analyses. Interestingly, most cell arrests in collecting venules (92 of 147, or 63% of arrested cells) occurred within two vessel diameters of vascular junctions, suggesting hotspots for the recruitment of HPCs in the BM. Although the average diameters and centerline velocities (V_{max}) were lower in sinusoids than in collecting venules (Table 1, P < 0.05), the shear rates were similar between these two groups of microvessels. The mean percentage of rolling human CD34⁺ cells (~22%), similar to that described for a murine cell line and fetal liver progenitor cells in the BM of C57BL/6 mice (17), indicates that human CD34⁺ cells can efficiently interact with NOD/SCID BM microvessels.

P- and E-selectins are required for human CD34⁺ cell rolling in BM microvessels and homing to the BM compartment. Previous studies have suggested important roles for P- and E-selectins and VCAM-1 in mouse progenitor homing to the BM, and that each pathway (VCAM-1/β1 integrin and selectin/mucin ligands) contributes equally to recruitment of mouse HPCs (15–18). To evaluate the role of endothelial selectins and VCAM-1 in the initial interactions of human CD34⁺ cells with BM microvessels, we backcrossed the P- and E-selectin mutations into the NOD/SCID background and used an mAb (MK 2.7) to inhibit VCAM-1 function. CD34⁺ cells were purified from MNCs prepared from mPB samples and fluorescently labeled with CFSE. Mice were preinjected with either an anti–VCAM-1 Ab (MK 2.7) or rat IgG control prior to the injection of CD34⁺ cells. Anti–VCAM-1 administration reduced CD34⁺ cell rolling by about 33% (P = 0.05) in the BM microvasculature of wild-type NOD/SCID mice, compared with IgG injection or no injection (Figure 3). Strikingly, CD34⁺ cell rolling was drastically reduced (~95% reduction) in BM microvessels of P/E$^{-/-}$ NOD/SCID mice preinjected with either IgG or anti–VCAM-1 (Figure 3). These differences were not due to alterations in hemodynamics of the BM microcirculation since there was no difference in the shear

Table 1
Hemodynamic characteristics of BM microvessels

Mice	Source of	No. of			Vessel diameter (μm)			V_{max} (μm/s)			WSR (s^{-1})		
	CD34 cells	Cv	S	Mice	Cv	S	Cv⁺S	Cv	S	Cv⁺S	Cv	S	Cv⁺S
NOD/SCID	mPB	30	30	10	49 ± 3	28 ± 2[A]	38 ± 2	3,731 ± 390	1,578 ± 146[A]	2,655 ± 249	321 ± 40	245 ± 21	283 ± 23
	CB	17	30	8	47 ± 3	32 ± 1[A]	40 ± 3	3,206 ± 233	1,625 ± 166[A]	2,762 ± 347	283 ± 22	216 ± 20[A]	297 ± 27
	BM	15	18	7	54 ± 4	29 ± 2[A]	37 ± 2	3,681 ± 640	1,997 ± 242[A]	2,197 ± 174	309 ± 42	287 ± 37	240 ± 16
N/S WT	mPB	18	23	5	42 ± 2	26 ± 1[A]	33 ± 2	3,050 ± 476	1,326 ± 147[A]	2,224 ± 296	295 ± 49	222 ± 26	272 ± 30
N/S PE$^{-/-}$	mPB	9	23	5	49 ± 3	30 ± 2[A]	35 ± 2	3,201 ± 561	1,555 ± 211[A]	2,018 ± 251	259 ± 41	252 ± 28	254 ± 23
N/S E$^{-/-}$	CB	19	14	7	41 ± 3	32 ± 1[A]	37 ± 2	1,873 ± 182	1,267 ± 159[A]	1,619 ± 134	234 ± 28	208 ± 29	223 ± 20

The velocity of free-flowing cells (V_{max}) was determined in collecting venules (Cv) and sinusoids (S) after the injection of fluorescently labeled human erythrocytes or CD34⁻ cells. Vessel diameters were measured using a video caliper, and wall shear rates (WSRs) were calculated as described in Methods. Data are arithmetic mean ± SEM. [A] P < 0.05 compared with Cv. N/S WT, backcrossed wild-type NOD/SCID; N/S PE$^{-/-}$, P- and E-selectin–deficient NOD/SCID; N/S E$^{-/-}$, E-selectin–deficient NOD/SCID.

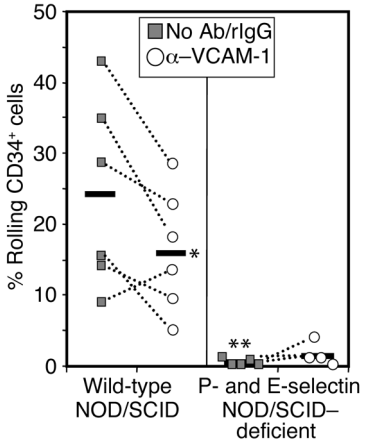

Figure 3
Role of P- and E-selectins and VCAM-1 in the initial interactions of human CD34$^+$ cells with BM microvessels. Fluorescently labeled human CD34$^+$ cells purified from mPB were injected into P/E$^{-/-}$ or wild-type mice backcrossed into the NOD/SCID background. Mice were injected via carotid catheter with control rat IgG (or no Ab in two experiments) and then with labeled CD34$^+$ cells. After 15 minutes of recording, fluorescent cells were completely cleared from the circulation. The same mouse was then injected with anti–VCAM-1 and a second bolus of fluorescent CD34$^+$ cells. Horizontal bars represent mean values. Each dot represents a single experiment before (filled squares) or after anti–VCAM-1 injection (open circles). *P = 0.05 by paired Student t test; **P = 0.003 by unpaired Student t test compared with IgG group in wild-type animals.

rate between the two groups of mice (Table 1). These results indicate that, in contrast to murine progenitors (16, 17), the initial interactions of human CD34$^+$ cells are largely dependent on endothelial selectins that are constitutively expressed in the BM tissue and that VCAM-1 plays a partial role in this activity.

To determine whether the defect in the initial interactions of human CD34$^+$ cells in P/E$^{-/-}$ NOD/SCID mice prevents extravasation into the BM compartment (i.e., homing), unsorted MNCs from mPB were injected into wild-type or P/E$^{-/-}$ NOD/SCID mice. Homed human cells were detected by FACS analysis using species-specific Ab's against CD34 and CD45 (Figure 4, a and b). Homing of CD34$^+$/CD45$^+$ human cells was reduced by approximately 90% in P/E$^{-/-}$ mice compared with wild-type animals (Figure 4, c–e). Of note, CD45$^+$CD34$^-$ lymphocytes also lodged in the BM of NOD/SCID mice 2 hours after their injection (Figure 4c, lower region), suggesting that donor lymphocytes also rapidly home to the recipient BM after transplantation. However, the numbers of lymphocytes were only modestly reduced (39%, P = 0.02) in the BM of P/E$^{-/-}$ animals (Figure 4d). Taken together, our intravital observations and the results from the short-term homing assays indicate that endothelial selectins are necessary for human CD34$^+$ cell rolling on BM microvessels and homing into the BM compartment of NOD/SCID mice.

Defective interactions of CB-derived CD34$^+$ cells with BM microvessels. Human HPCs can be routinely harvested for clinical transplantation from three different sources, including the BM, mPB, and CB. To evaluate differential homing mechanisms of human HPCs, we isolated CD34$^+$ cells from fresh samples obtained from these three sources. Fluorescently labeled CD34$^+$ cells were injected via a carotid artery catheter, and their interactions in the contralateral midparietal BM were recorded. Detailed analyses of videotapes revealed that the mean percentages of rolling and arrested cells in NOD/SCID BM microvessels were similar between mPB- and BM-derived CD34$^+$ cells (Figure 5). However, the interactions of CB-derived CD34$^+$ cells were significantly altered (~50% and ~60% reduction for rolling and arrested cells, respectively) compared with those derived from adult sources (Figure 5). Hemodynamic parameters were similar among the three groups (Table 1). These results suggest a defect in the capacity of neonate-derived CD34$^+$ cells to interact with the endothelium of BM microvessels.

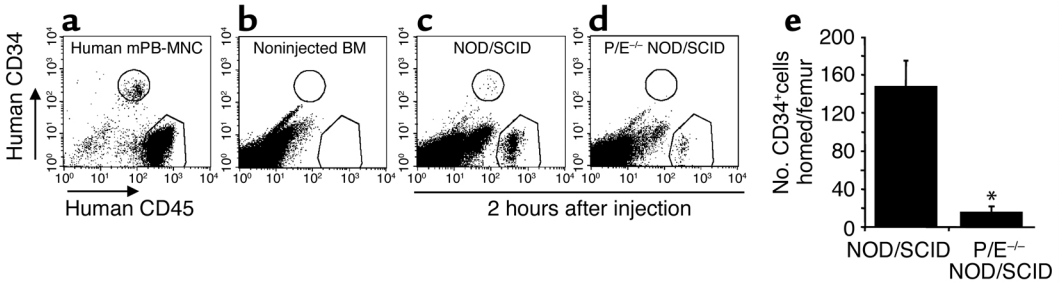

Figure 4
Role of P- and E-selectins in the homing of human CD34$^+$ cells to the BM of NOD/SCID mice. Sublethally irradiated NOD/SCID or P/E$^{-/-}$ NOD/SCID mice were injected intravenously with 2×10^7 human MNCs from mPB samples. Cells were allowed to home for 2 hours, and the femoral BM was harvested. (**a**) Double staining of the transplanted human MNCs for human CD34 and CD45. (**b**) BM cells recovered from an uninjected control mouse stained for human CD34 and CD45. (**c**) Wild-type NOD/SCID mouse transplanted with human MNCs. (**d**) P/E$^{-/-}$ NOD/SCID mouse transplanted with human MNCs. (**e**) Number of human CD34$^+$ cells homed per femur in transplanted wild-type NOD/SCID and P/E$^{-/-}$ NOD/SCID mice. The percentage of gated CD34$^+$/CD45$^+$ human cells (upper region in the scattergrams in **c**–**d**) in the recipient BM was determined by FACS analysis, and the number of homed cells per femur was calculated based on the femoral cellularity. The number of homed human CD34$^+$ cells is drastically reduced in P/E$^{-/-}$ NOD/SCID mice. n = 6 mice injected with MNCs from two different human donors. *P = 0.0008.

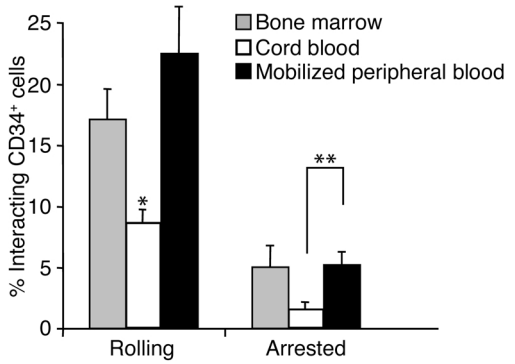

Figure 5
Comparative analysis of the interactions of CD34⁺ cells with BM microvessels in NOD/SCID mice. Fluorescently labeled CD34⁺ cells from steady-state human BM, mPB, or CB were injected into NOD/SCID mice, and the numbers of cells interacting (rolling or arrested) with the BM microvasculature were determined by analysis of video recordings from fluorescence intravital microscopy experiments. n = 7–10 mice and human donors. *$P < 0.02$ compared with BM and mPB. **$P = 0.03$.

Neonate-derived CD34⁺ cell binding to soluble P-selectin, but not soluble E-selectin, is impaired. Since endothelial selectins are required for rolling of CD34⁺ cells (Figure 3), the lower rolling numbers of CB CD34⁺ cells suggested a reduced expression or function of selectin ligands on neonatal progenitor cells. To evaluate this possibility, we tested the ability of CB- and mPB-derived CD34⁺ cells to bind P-selectin or E-selectin in a fluid-phase assay. Mononuclear cells were isolated from fresh mPB and CB samples and stained with anti-CD34 and the human P-selectin–IgG chimera in the presence and absence of divalent cations. Eight individual donor pair samples were thus prepared in parallel and evaluated by FACS analysis. As shown in Figure 6a, the geometric mean of fluorescence of P-selectin–IgG binding among CD34⁺ cells was 59% lower in CB than in mPB ($P = 0.008$). Binding was specific since it was abrogated in divalent cation–chelated samples (Figure 6, a and b). Analysis of flow cytometry scattergrams revealed that while the vast majority (90% ± 1%) of mPB CD34⁺ cells bound P-selectin–IgG, approximately one-third of CB-derived CD34⁺ cells (34% ± 3%) did not bind soluble P-selectin (Figure 6b), suggesting a defect in expression or function of P-selectin ligand on a subpopulation of CB CD34⁺ cells. This finding was not exclusive to the human P-selectin chimeric construct since similar results were obtained with murine P-selectin–IgM (data not shown). To evaluate the function of E-selectin ligands, we analyzed the binding of a murine E-selectin–IgM chimera to purified adult and neonatal CD34⁺ cells. In contrast to P-selectin binding, only 60–70% of CD34⁺ cells bound E-selectin–IgM, but there was no significant difference in binding between CB and mPB (68% ± 2% and 62% ± 6% for CB and mPB CD34⁺ cells, respectively; $n = 6$, $P = 0.33$). These data indicate that function or expression of P-selectin ligands, but not E-selectin ligands, is significantly altered on neonate-derived CD34⁺ cells.

Because PSGL-1 has been reported to be the main functional receptor for P-selectin in BM-derived CD34⁺ cells (24), we analyzed its expression. Using two different mAb's against PSGL-1 (PSL-275 and KPL1), we found that most adult and neonatal CD34⁺ cells expressed this antigen (94% ± 2% in CB and 97% ± 1% in mPB, $n = 5$) (Figure 6c). To investigate whether PSGL-1 is the main functional P-selectin ligand on mPB and CB CD34⁺ cells, MNCs were stained with

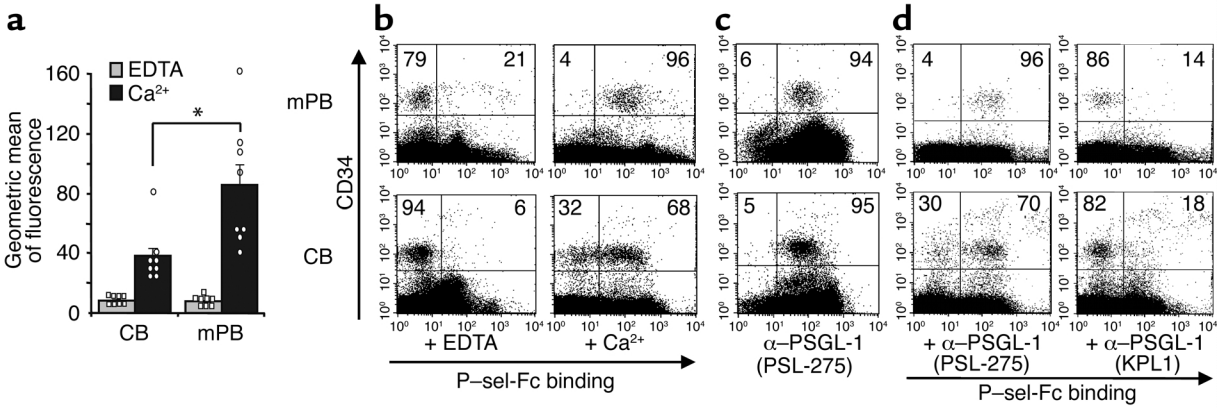

Figure 6
Binding of soluble P-selectin and PSGL-1 expression on CB and mPB CD34⁺ cells. (**a**) MNCs obtained from CB or mPB samples were stained for CD34 and P-selectin–IgG binding in the presence or absence of 5 mM EDTA. Data represent geometric mean of fluorescence ± SEM of P-selectin–IgG binding on gated CD34⁺ cells. $n = 8$ separate experiments from different donors. *$P = 0.008$. (**b**) Scattergram profiles of CB and mPB MNCs stained for CD34⁺ cells and P-selectin–IgG in the presence or absence of 5 mM EDTA. In the presence of divalent cations, virtually all mPB CD34⁺ cells bind P-selectin–IgG, whereas two distinct subpopulations are present among CB CD34⁺ cells: one that binds P-selectin–IgG normally (~70%) and one that does not bind soluble P-selectin (~30%). (**c**) Expression of PSGL-1 in CB and mPB CD34⁺ cells. (**d**) PSGL-1 is the sole P-selectin ligand on CB and mPB CD34⁺ cells. MNCs were preincubated with 2 μg of function-blocking (KPL1) or non-blocking (PSL-275) anti–PSGL-1 before staining to detect P-selectin–IgG chimera binding and CD34. The numbers indicate the percentage of CD34⁺ cells in each quadrant. The scattergrams represent one of at least five replicates.

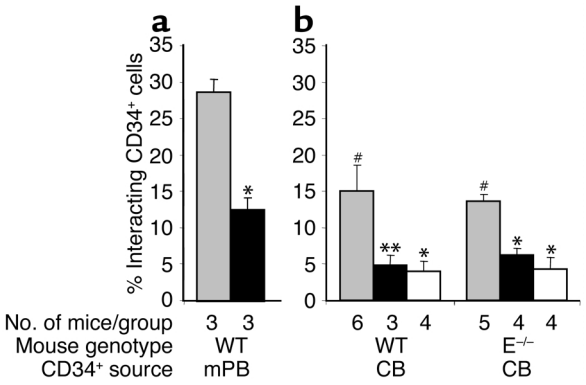

Figure 7
Role of P-selectin and PSGL-1 in CD34$^+$ cell interactions with BM microvessels. Fluorescently labeled CD34$^+$ cells from mPB (**a**) or CB (**b**) were preincubated with anti–PSGL-1 (black bars) or isotype-matched control Ab and injected into wild-type or E$^{-/-}$ NOD/SCID mice that had been treated with anti–P-selectin (white bars) or isotype-matched control Ab (gray bars). The number of cells interacting with the BM microvasculature was determined by analysis of video recordings from fluorescence intravital microscopy experiments. *P < 0.02 compared with control Ab; **P = 0.06 compared with control Ab; $^{\#}P$ < 0.02 compared with mPB control Ab group shown in **a**.

anti-CD34 Ab and incubated with either function-blocking (KPL1) or non-blocking (PSL-275) mAb against PSGL-1 prior to evaluating soluble P-selectin binding. Preincubation of cells with KPL1, but not with PSL-275, almost completely inhibited P-selectin–IgG binding in both CB- and mPB-derived CD34$^+$ cells (Figure 6d). The normal expression of PSGL-1 glycoprotein on CB CD34$^+$ cells, together with the evidence of abnormal function in a subset of CD34$^+$ cells, suggests defective posttranslational modifications of the PSGL-1 protein in a subpopulation of CB CD34$^+$ cells.

The PSGL-1/P-selectin pathway plays a major role in the initial interactions of CD34$^+$ cells with BM microvessels. To assess whether PSGL-1 mediates CD34$^+$ cell rolling in vivo, we treated fluorescently labeled mPB CD34$^+$ cells with anti–PSGL-1 or control IgG and evaluated their behavior in the BM microcirculation after intracarotid injection. As shown in Figure 7a, the number of rolling CD34$^+$ cells was significantly lower (~56% reduction) in the group treated with anti–PSGL-1. To further test whether the reduced rolling capacity of CB-derived CD34$^+$ cells might be due to defective PSGL-1, we tested the individual roles of PSGL-1, P-selectin, and E-selectin using E$^{-/-}$ mice backcrossed in the NOD/SCID background and inhibitory Ab's against P-selectin and PSGL-1. We found that the reduction observed earlier (Figure 3) in CB CD34$^+$ cell rolling compared with cells derived from mPB was similar in wild-type NOD/SCID and E$^{-/-}$ NOD/SCID mice (Figure 7b). However, inhibition of P-selectin function in both wild-type and E$^{-/-}$ NOD/SCID mice greatly reduced (by 74% and 68%, respectively) the number of rolling CB CD34$^+$ cells in the BM microvasculature (Figure 7b). In addition, blockage of PSGL-1 function on CB CD34$^+$ cells inhibited their interactions in both wild-type and E-selectin–deficient mice (68% and 55% reduction, respectively). Inhibition using an anti–E-selectin Ab (clone 9A9) produced similar results to E-selectin deficiency (n = 2, data not shown). These data indicate that the PSGL-1/P-selectin pathway plays a major role in initial interactions and strongly suggest that the reduced ability of CB CD34$^+$ cells to interact with the BM microvessels is due to altered P-selectin binding.

Neonatal CD34$^+$ cells defective in P-selectin binding are enriched in primitive CD34$^+$CD38$^{lo/-}$ cells. CD34$^+$ cells represent a heterogeneous population of progenitors with various degrees of hematopoietic maturation. The lack or dim expression of CD38 in human CD34$^+$ cells is considered to be a surrogate marker of their primitive nature (25). To further characterize the population of CB-derived CD34$^+$ cells that do not bind P-selectin–IgG, we analyzed P-selectin chimera binding and CD38 expression among CD34$^+$ cells. As shown in Figure 8, CD34$^+$ cells that did not bind P-selectin–IgG (Figure 8a, region in red) contained 23% ± 3% CD38$^{lo/-}$ cells, compared with only 9% ± 1% CD34$^+$ cells that bound soluble P-selectin (Figure 8b, region in green; n = 8 different donors, P = 0.0006). Thus, CD34$^+$ progenitors that do not bind P-selectin are enriched in primitive HPCs.

Engraftment of NOD/SCID mice by CB CD34$^+$ cells is not compromised. To determine whether the defect of CB CD34$^+$ cell rolling might influence their engraftment into NOD/SCID mice, CD34$^+$ cells were purified from CB and healthy mPB donors and transplanted into sublethally irradiated (350–375 cGy) NOD/SCID animals or NOD/SCID mice deficient in β2 microglobulin. One month after transplantation, mice were sacrificed to assess the engraftment levels of human-derived progenitors. As shown in Figure 9, there was a trend toward higher engraftment levels in the CB group compared with the mPB group, as measured by the frequency of human CD45$^+$ cells and human progenitors in the BM compartment. These data are

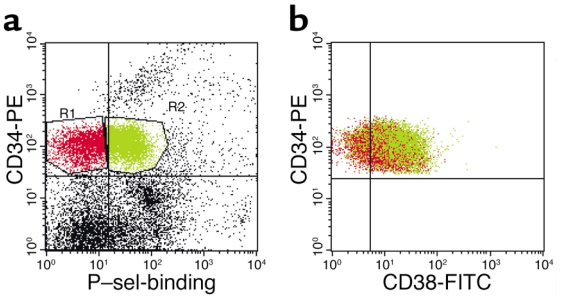

Figure 8
Reduced binding of soluble P-selectin on primitive neonatal HPCs (CD34$^+$CD38$^{lo/-}$). MNCs obtained from CB samples were stained for CD34 (using PE) and CD38 (using FITC) expression, and P-selectin–IgG chimera binding (using Cy5). (**a**) The gated regions represent CD34$^+$ cells that bind (R2, green) or do not bind (R1, red) P-selectin–IgG. (**b**) CD38 expression on cells from R1 and R2 regions. The majority of cells that do not bind P-selectin–IgG are primitive CD34$^+$CD38$^{lo/-}$ cells. Shown is one representative of eight replicates.

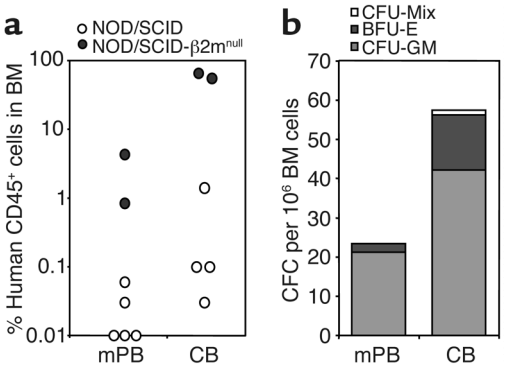

Figure 9
Engraftment of CB CD34$^+$ cells in NOD/SCID mouse BM is not compromised. CD34$^+$ cells isolated from CB or healthy mPB donors were transplanted into sublethally irradiated (350–375 cGy) NOD/SCID animals or NOD/SCID mice deficient in β2 microglobulin (NOD/SCID-β2m^{null}). Four weeks after transplantation, mice were sacrificed to assess the levels of human-derived CD45$^+$ cells (**a**) or colony-forming progenitors (**b**) in their BM. There is a trend toward higher engraftment of CB-derived CD34$^+$ cells (P = 0.07 for CD45$^+$ and P = 0.1 for CFC content). Each circle in **a** represents an individual mouse.

consistent with those of Wang et al., who found a higher level of engraftment of CB MNCs than of either BM or mPB MNCs (26), and suggest that CB CD34$^+$ cells can compensate for their reduced initial interactions with the BM endothelium.

Discussion

The BM microvasculature differs from that of other tissues in several aspects. For example, the BM compartment does not contain capillaries but is endowed with a rich sinusoidal network. The fenestrated endothelium lining BM sinusoids promotes the release of billions of blood cells each day. Yet hematopoietic progenitors and mature blood cells (for example, B lymphocytes) likely reenter the BM under homeostatic conditions, and such trafficking is critical during hematopoietic development and BM transplantation. Because collecting venules mediate the recruitment of mature leukocytes during inflammation, we initially analyzed whether human HPCs interacted preferentially with sinusoids or collecting venules. We found that the two vessel types recruited circulating progenitors equally well. It is interesting that a high frequency of cell arrest was mapped within two vessel diameters of venular junctions, suggesting preferential endothelial areas for the recruitment of CD34$^+$ cells. It is possible that these hotspots reflect differential endothelial adhesion molecule or chemokine expression in areas of nonlaminar blood flow. For example, alterations in shear stress can upregulate ICAM-1 and VCAM-1 expression (27). Although the numbers of rolling and arrested HPCs were similar between sinusoids and collecting venules, the majority of HPCs may in fact use sinusoids for BM homing, since the overall surface area of BM sinusoids is likely larger (28).

Strikingly, human CD34$^+$ cell rolling was virtually absent in BM microvessels lacking P- and E-selectins. Endothelial selectins play a critical function in the recruitment of mature leukocytes (7, 8), but only a partial role (50% reduction) for P- and E-selectins was found in murine progenitor cell rolling (17) and homing (16) in the BM. Near-complete inhibition of HPC homing was achieved by blocking VCAM-1 function in selectin-deficient mice in both assay systems. In contrast to the studies with murine progenitors, we found that both rolling of human CD34$^+$ cells on BM microvessels and homing to the NOD/SCID mouse BM were almost completely dependent on the expression of P- and E-selectin. Even if VCAM-1 inhibition significantly reduced the number of rolling cells, our results suggest that VCAM-1 cannot compensate when endothelial selectins are absent.

It is important to note that although the human α4 integrin (VLA-4) and human PSGL-1 have been shown to bind mouse VCAM-1 and mouse P-selectin, respectively, we cannot exclude the possibility that a difference in the affinities of human adhesion molecules for their respective murine counterreceptors may have influenced the results in this xenogeneic model. Our data are in agreement with those of Peled and colleagues, who found that a density of immobilized P- or E-selectin lower than the density of immobilized VCAM-1 could mediate human CD34$^+$ cell tethering under physiological flow in vitro (29), suggesting that human CD34$^+$ cells preferentially interact with endothelial selectins. However, blockade of the VLA-4 integrin (the ligand of VCAM-1) significantly inhibited the migration of human CD34$^+$ cells into fetal sheep BM (30).

It is likely that VLA-4 integrin, a versatile receptor that can mediate both cell-cell (via VCAM-1) and cell-matrix (via fibronectin) interactions (31), operates at each step involved in HPC homing, including rolling, arrest, and migration. The modest effect of VCAM-1 inhibition in our studies argues that VLA-4 may act primarily at the latter steps of the homing cascade (arrest and migration), in which fibronectin plays important roles. Because selectin interactions with their ligands produce slow rolling and can induce signaling, it is also conceivable that the interactions of HPCs with endothelial selectins may enhance VLA-4's affinity by increasing the contact of HPCs with immobilized chemokines on the endothelial surface, or perhaps by selectin ligand–mediated "inside-out" signaling (29, 32).

Blockade of adhesion molecules involved in the interaction of cells with extracellular matrix molecules (ECMs) can also alter progenitor behavior in vivo. For example, homing to the BM of β1 integrin–deficient murine progenitors is severely compromised (33), and blockade of either one of the two major β1 integrins (α4 and α5) on human CB progenitors was shown to inhibit migration through ECM and engraftment in NOD/SCID mice (34). These results, together with those of our colleagues, highlight the importance of

two critical and largely nonoverlapping pathways for human HPC homing in which the initial interactions are mediated by endothelial selectins, while β1 integrins are largely involved in the subsequent steps.

Since human hematopoietic progenitors can be obtained from three different sources for transplantation, we sought to comparatively evaluate whether the hematopoietic milieu from which $CD34^+$ cells were harvested might influence their behavior in vivo. Using our intravital microscopy system, we found that the number of rolling neonate-derived $CD34^+$ cells in the BM of NOD/SCID mice was significantly reduced compared with those of adult $CD34^+$ cells obtained either from steady-state BM or mPB. Because endothelial selectins mediate HPC rolling (Figure 3), we assessed the function of selectin ligands on $CD34^+$ cells. Binding of soluble P-selectin was reduced in a subset of neonatal $CD34^+$ cells compared with binding in HPCs derived from adult subjects.

A defect in the posttranslational processing of PSGL-1 protein was suggested by two observations: PSGL-1 is expressed on all CB $CD34^+$ cells (Figure 6c), but a subset of these cells do not bind P-selectin; and PSGL-1 is the sole P-selectin ligand on $CD34^+$ cells obtained from either steady-state BM (24), neonatal blood (ref. 29 and this study), or mPB (Figure 6d). Our results suggest that the reduced interactions of CB-derived $CD34^+$ cells are due to surface expression of nonfunctional PSGL-1, since the PSGL-1/P-selectin pathway plays a major role in $CD34^+$ cell rolling in vivo. Although the molecular defect responsible for defective PSGL-1 function in the subset of CB-derived $CD34^+$ cells remains to be defined, specific posttranslational modifications in the PSGL-1 polypeptide have been well described for mature leukocytes, including sialylation, fucosylation, and tyrosine sulfation (13).

Interestingly, Mariscalco and colleagues found that neonatal neutrophil rolling on monolayers of Chinese hamster ovary (CHO) cells transfected with P-selectin was reduced compared with that of adult neutrophils (35). Further studies are needed to characterize PSGL-1's defect(s) in both mature and immature neonatal cells. It is also noteworthy that P-selectin was shown to be absent in endothelial cells of newborn rat mesentery and decreased in newborn human mesentery (36). It is thus tempting to speculate that the P-selectin/PSGL-1 adhesion pathway is not fully functional during fetal life and may become operative only in the postnatal period.

Since the fraction of neonatal $CD34^+$ cells that does not bind P-selectin is enriched in primitive $CD34^+CD38^{lo/-}$ cells, our findings may have important implications for clinical BM transplantation. Neonatal blood has been used as a source of HPCs in more than 1,500 cases of transplantation thus far (37). Although CB-derived progenitors offer several advantages over those harvested from adult sources, including wide availability, ease of harvest, and lower incidence of graft-versus-host disease, the limited number of cells recovered per unit has restricted transplantation mostly to individuals with low body weights (i.e., children) (22). Significant delays in platelet and myeloid engraftment have been reported in CB cell transplantation (22, 38). It is unclear, however, whether this is due to low numbers of transplanted HPCs or a defect in homing. Our results indicate that although homing of CB $CD34^+$ cells is impaired, their engraftment is at least as high as that of adult $CD34^+$ cells. Thus, these data raise the possibility that the defect in the initial interactions of CB $CD34^+$ cells in the BM microcirculation may be compensated for by other "youthful" characteristics of neonatal cells. For example, CB progenitors have a greater proliferation and expansion capacity (26, 39) and a greater proportion of immature $CD34^+CD38^-$ cells than do their adult counterparts (40). In support of the present studies, while our manuscript was under review, Szilvassy et al. reported on a discrepancy between homing and engraftment of fetal liver progenitor cells (reduced homing and higher engraftment of fetal HPCs compared with BM- and mPB-derived HPCs) (41). Greater insights into the mechanisms and regulation of PSGL-1's posttranslational modifications in neonatal cells may thus allow us to optimize the initial interactions of CB-derived stem cells with endothelial cells, and to enhance their lodgement in the BM. Our results indeed underscore the enormous potential of CB cells as a source of hematopoietic stem cells.

Acknowledgments

We thank Steve Fruchtman, Luis Isola, and the Stem Cell Lab staff for help in procuring human adult hematopoietic samples, and the Labor and Delivery team at Mount Sinai Medical Center for assistance in obtaining neonatal blood. We thank Robert S. Schaub, John Lowe, Barry Wolitzky, and Masaru Okabe for providing reagents. We also thank Seunghee Kim-Schulze for help in the initial experiments and Yoshio Katayama for helpful discussions. These studies were funded in part by a scholarship from the American Society of Hematology and the National Institutes of Health (R01 DK-56638) to P.S. Frenette.

1. Jacobson, L.O., Marks, E.K., Robson, M.J., Gaston, E., and Zirkle, R.E. 1949. The effect of spleen protection on mortality following X-radiation. *J. Lab. Clin. Med.* **34**:1538–1543.
2. Lorenz, E., Uphoff, D., Reid, T.R., and Shelton, E. 1951. Modification of irradiation injury in mice and guinea pigs by bone marrow injections. *J. Natl. Cancer Inst.* **12**:197–201.
3. Barnes, D.W.H., Corp, M.J., Loutit, J.F., and Neal, F.E. 1956. Treatment of murine leukaemia with x-rays and homologous bone marrow. Preliminary communication. *Br. Med. J.* **2**:626–627.
4. Thomas, E.D. 1995. History, current results, and research in marrow transplantation. *Perspect. Biol. Med.* **38**:230–237.
5. Frenette, P.S., and Wagner, D.D. 1996. Adhesion molecules—Part II: Blood vessels and blood cells. *N. Eng. J. Med.* **335**:43–45.
6. Kansas, G.S. 1996. Selectins and their ligands: current concepts and controversies. *Blood.* **88**:3259–3287.
7. Frenette, P.S., Mayadas, T.N., Rayburn, H., Hynes, R.O., and Wagner, D.D. 1996. Susceptibility to infection and altered hematopoiesis in mice deficient in both P- and E-selectins. *Cell.* **84**:563–574.
8. Bullard, D.C., et al. 1996. Infectious susceptibility and severe deficiency of leukocyte rolling and recruitment in E-selectin and P-selectin double mutant mice. *J. Exp. Med.* **183**:2329–2336.

9. Moore, K.L., et al. 1992. Identification of a specific glycoprotein ligand for P-selectin (CD62) on myeloid cells. *J. Cell Biol.* **118**:445–456.
10. Frenette, P.S., et al. 2000. P-Selectin glycoprotein ligand 1 (PSGL-1) is expressed on platelets and can mediate platelet-endothelial interactions in vivo. *J. Exp. Med.* **191**:1413–1422.
11. Zannettino, A.C., et al. 1995. Primitive human hematopoietic progenitors adhere to P-selectin (CD62P). *Blood.* **85**:3466–3477.
12. Tracey, J.B., and Rinder, H.M. 1996. Characterization of the P-selectin ligand on human hematopoietic progenitors. *Exp. Hematol.* **24**:1494–1500.
13. Moore, K.L. 1998. Structure and function of P-selectin glycoprotein ligand-1. *Leuk. Lymphoma.* **29**:1–15.
14. Springer, T.A. 1995. Traffic signals on endothelium for lymphocyte recirculation and leukocyte emigration. *Annu. Rev. Physiol.* **57**:827–872.
15. Papayannopoulou, T., Craddock, C., Nakamoto, B., Priestley, G.V., and Wolf, N.S. 1995. The VLA4/VCAM-1 adhesion pathway defines contrasting mechanisms of lodgement of transplanted murine hemopoietic progenitors between bone marrow and spleen. *Proc. Natl. Acad. Sci. USA.* **92**:9647–9651.
16. Frenette, P.S., Subbarao, S., Mazo, I.B., von Andrian, U.H., and Wagner, D.D. 1998. Endothelial selectins and vascular cell adhesion molecule-1 promote hematopoietic progenitor homing to bone marrow. *Proc. Natl. Acad. Sci. USA.* **95**:14423–14428.
17. Mazo, I.B., et al. 1998. Hematopoietic progenitor cell rolling in bone marrow microvessels: parallel contributions by endothelial selectins and VCAM-1. *J. Exp. Med.* **188**:465–474.
18. Vermeulen, M., et al. 1998. Role of adhesion molecules in the homing and mobilization of murine hematopoietic stem and progenitor cells. *Blood.* **92**:894–900.
19. Shultz, L.D., et al. 1995. Multiple defects in innate and adaptative immunologic function in NOD/LtSz-scid mice. *J. Immunol.* **154**:180–191.
20. Dick, J.E., Bhatia, M., Gan, O., Kapp, U., and Wang, J.C. 1997. Assay of human stem cells by repopulation of NOD/SCID mice. *Stem Cells.* **15**(Suppl. 1):199–203; discussion 204–207.
21. Rocha, V., et al. 2001. Comparison of outcomes of unrelated bone marrow and umbilical cord blood transplants in children with acute leukemia. *Blood.* **97**:2962–2971.
22. Rubinstein, P., et al. 1998. Outcomes among 562 recipients of placental-blood transplants from unrelated donors. *N. Engl. J. Med.* **339**:1565–1577.
23. Maly, P., et al. 1996. The alpha(1,3)fucosyltransferase Fuc-TVII controls leukocyte trafficking through an essential role in L-, E-, and P-selectin ligand biosynthesis. *Cell.* **86**:643–653.
24. Levesque, J.P., et al. 1999. PSGL-1-mediated adhesion of human hematopoietic progenitors to P-selectin results in suppression of hematopoiesis. *Immunity.* **11**:369–378.
25. Terstappen, L.W., Huang, S., Safford, M., Lansdorp, P.M., and Loken, M.R. 1991. Sequential generations of hematopoietic colonies derived from single nonlineage-committed $CD34^+CD38^-$ progenitor cells. *Blood.* **77**:1218–1227.
26. Wang, J.C., Doedens, M., and Dick, J.E. 1997. Primitive human hematopoietic cells are enriched in cord blood compared with adult bone marrow or mobilized peripheral blood as measured by the quantitative in vivo SCID-repopulating cell assay. *Blood.* **89**:3919–3924.
27. Walpola, P.L., Gotlieb, A.I., Cybulsky, M.I., and Langille, B.L. 1995. Expression of ICAM-1 and VCAM-1 and monocyte adherence in arteries exposed to altered shear stress. *Arterioscler. Thromb. Vasc. Biol.* **15**:2–10.
28. Lichtman, M.A. 1981. The ultrastructure of the hemopoietic environment of the marrow: a review. *Exp. Hematol.* **9**:391–410.
29. Peled, A., et al. 1999. The chemokine SDF-1 stimulates integrin-mediated arrest of $CD34^+$ cells on vascular endothelium under shear flow. *J. Clin. Invest.* **104**:1199–1211.
30. Zanjani, E.D., Flake, A.W., Almeida-Porada, G., Tran, N., and Papayannopoulou, T. 1999. Homing of human cells in the fetal sheep model: modulation by antibodies activating or inhibiting very late activation antigen-4-dependent function. *Blood.* **94**:2515–2522.
31. Masumoto, A., and Hemler, M.E. 1993. Multiple activation states of VLA-4. Mechanistic differences between adhesion to CS1/fibronectin and to vascular cell adhesion molecule-1. *J. Biol. Chem.* **268**:228–234.
32. Lorenzon, P., et al. 1998. Endothelial cell E- and P-selectin and vascular cell adhesion molecule-1 function as signaling receptors. *J. Cell Biol.* **142**:1381–1391.
33. Potocnik, A.J., Brakebusch, C., and Fassler, R. 2000. Fetal and adult hematopoietic stem cells require beta1 integrin function for colonizing fetal liver, spleen, and bone marrow. *Immunity.* **12**:653–663.
34. Peled, A., et al. 2000. The chemokine SDF-1 activates the integrins LFA-1, VLA-4, and VLA-5 on immature human $CD34^{(+)}$ cells: role in transendothelial/stromal migration and engraftment of NOD/SCID mice. *Blood.* **95**:3289–3296.
35. Mariscalco, M.M., Tcharmtchi, M.H., and Smith, C.W. 1998. P-Selectin support of neonatal neutrophil adherence under flow: contribution of L-selectin, LFA-1, and ligand(s) for P-selectin. *Blood.* **91**:4776–4785.
36. Lorant, D.E., Li, W., Tabatabaei, N., Garver, M.K., and Albertine, K.H. 1999. P-selectin expression by endothelial cells is decreased in neonatal rats and human premature infants. *Blood.* **94**:600–609.
37. Gluckman, E. 2001. Hematopoietic stem-cell transplants using umbilical-cord blood. *N. Engl. J. Med.* **344**:1860–1861.
38. Barker, J.N., et al. 2001. Survival after transplantation of unrelated donor umbilical cord blood is comparable to that of human leukocyte antigen-matched unrelated donor bone marrow: results of a matched-pair analysis. *Blood.* **97**:2957–2961.
39. Mayani, H., and Lansdorp, P.M. 1998. Biology of human umbilical cord blood-derived hematopoietic stem/progenitor cells. *Stem Cells.* **16**:153–165.
40. Cardoso, A.A., et al. 1993. Release from quiescence of $CD34^+$ CD38- human umbilical cord blood cells reveals their potentiality to engraft adults. *Proc. Natl. Acad. Sci. USA.* **90**:8707–8711.
41. Szilvassy, S.J., Meyerrose, T.E., Ragland, P.L., and Grimes, B. 2001. Differential homing and engraftment properties of hematopoietic progenitor cells from murine bone marrow, mobilized peripheral blood, and fetal liver. *Blood.* **98**:2108–2115.